Eur. Phys. J. B **46**, 127–132 (2005)
DOI: 10.1140/epjb/e2005-00238-8

THE EUROPEAN PHYSICAL JOURNAL B

Electromagnetic-field-induced resonant structures for an open rectangular quantum dot

Guanghui Zhou[1,2,3,a] and Yuan Li[2]

[1] CCAST (World Laboratory), P.O. Box 8730, Beijing 100080, China
[2] Department of Physics, Hunan Normal University, Changsha 410081, China
[3] International Center for Materials Physics, Chinese Academy of Sciences, Shenyang 110015, China

Received 23 February 2005
Published online 8 August 2005 –

Abstract. We study theoretically the electron transport properties for an open rectangular quantum dot under an external electromagnetic field illumination in the ballistic regime. Using the effective mass free-electron approximation, the scattering matrix for the system has been formulated by the time-dependent mode-match method. Some interesting properties of the electron transmission have been demonstrated through serval numerical examples. The dependence of electron transmission on the electron incident energy is found to exhibit Fano dip structures due to the field-induced intersubband scatterings into quasibound states in the dot. Moreover, with an appropriate incident energy the electron transmission as a function of the field frequency and/or amplitude shows a rich structure. Our results suggest that the electron transport properties of an open rectangular quantum dot are affected by the interplay effects between the nonadiabatic dot-lead connection and the applied field.

PACS. 78.67.Hc Quantum dots – 73.23.Ad Ballistic transport – 71.10.Pm Fermions in reduced dimensions

1 Introduction

In recent years mesoscopic physics has been extensively studied due to its potential application in the future. Structures of a mesoscopic size, created in a two-dimensional electron gas (2DES) of a $GaAs/Al_xGa_{1-x}As$ semiconductor heterojunction using a split gate technique, have been a subject of intensive investigations during the last decade. In the ballistic regime and at low temperatures quantum coherent effects will dominate the electron transport in such mesoscopic systems. One of the most important features is that the conductance shows a histogram structure as the lateral size of a system varies, and each step has a height of $2e^2/h$ or integer multiples of it [1,2].

The electron transport properties of a quantum dot formed on a 2DEG can be affected by many factors. The presence of disorders results in a suppression of the conductance plateaus below the integer values [3], and the transmission behavior shows Fano resonance structures [4]. The interaction of electrons in the dot induces transport anomalies [5,6]. However, there has been growing interest in the time- and frequency-dependent responses of mesoscopic nanostructures in recent years. The time-modulation invoked are either high-frequency electromagnetic (EM) fields [7–13] or time-dependent bias potentials [14–16], or ac controlled gates [17]. There have been several interesting effects revealed in this kind of system, such as the mechanism of electron pumping [7], the photo-assisted processes [8], and the features of time-modulation-induced quasi-bound states [14].

Recently, the electron transport properties for an adiabatic dot-lead connected stadium-shape open quantum dot illuminated under a microwave has been investigated [14]. This system allows an electron mode in the lead to evolve in the dot. The situations occur when an electron in the lower mode in the dot can exit the dot without reflection, while an electron with the same incident energy but in a higher mode in the dot is trapped inside it. Therefore, intermode transitions between the two modes in the dot, as induced by the transversely polarized EM field, were found to result in resonant transmission blocking in a mesoscopic channel. Moreover, a nonadiabatic dot-lead connected rectangular shape open quantum dot modulated by a time-dependent bias potential has also been considered [16] and the quasibound state induced Fano structure resonances have been predicted. Fano resonance [18] is a very interesting phenomenon in quantum transport physics. If an absorbed impurity, [4] stub or any other geometry [17] producing localized states exists, Fano resonance caused by the interference between propagating state and bound state take place for a mesoscopic system.

An open quantum dot [19], consisting of a submicron sized cavity and quantum point contact leads, are ideally suited for studying the influence of environmental coupling on the discrete level spectrum of a quantum system. Of particular interest here is the nature of electron transport

[a] e-mail: ghzhou@hunnu.edu.cn

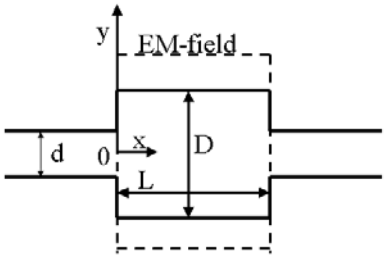

Fig. 1. The sketch of the system.

in open dot, whose leads are configured to support a small number of propagating modes. In this paper, we study the quantum transport properties of an open rectangular quantum dot illuminated under an external transversely polarized EM field. Our system is different from neither adiabatic dot-lead connect dot under a microwave illumination [11] nor the nonadiabatic dot-lead connected dot modulated by a time-dependent bias potential [16]. Using the effective mass free-electron approximation, the scattering matrix for the system has been formulated by the time-dependent mode-matching method. The electron transmission probability as a function of the incident energy, the field frequency and the field amplitude has been calculated. Although we have treated a simple model system, we have predicted some interesting new results which are distinguishable from the previous investigations [11,16] in several aspects. Firstly, there are some multiple Fano resonances due to the field-induced coupling among the modes in the dot. Secondly, one dip structure will occur when the two second modes in both dot and lead begin to be propagating simultaneously with appropriate external field parameters. Thirdly, we have expected a step structure if the second mode in the lead begin to be propagating earlier than the one in the dot. Up to our knowledge, these EM-field-induced effects have not been reported previously for the open rectangular quantum dot system.

The paper is organized as follows. In Section 2 we present the model and the method for formulating the scattering matrix of the system. In Section 3 we demonstrate some numerical examples illustrating the electron transport properties and discuss the results for the system. And finally, Section 4 gives a conclusion.

2 Model and method

The system under study is a two-dimensional rectangular open quantum dot with two leads connecting the electron reservoirs at each end. The dot with width D and length L is acted upon by an external transversely polarized EM field in an unspecified way, and the system is schematically depicted in Figure 1. The x-axis is longitudinally along the leads, and the y-axis describes the transversal direction. Assume that the field vector potential can be described as $\mathbf{A} = (\varepsilon/\omega)\cos(\omega t)\hat{e}_y$ with angular frequency ω and amplitude ε, where $\hat{e}_y$ is the unit vector in the polarized direction.

In the effective mass approximation, the single-particle time-dependent Schrödinger equation in the dot region reads

$$i\hbar\frac{\partial}{\partial t}\Psi(x,y,t) = \left[\frac{1}{2m*}\left(-\hbar^2\frac{\partial^2}{\partial x^2} + (i\hbar\frac{\partial}{\partial y} + eA)^2\right) + v_c(y)\right]\Psi(x,y,t), \quad (1)$$

where m^* is the effective electron mass and $v_c(y)$ is the transverse confining potential of the hard-wall type. In a real quantum dot, with nearby contacts and gates will induce spatially-dependent electric fields. However, here we start with a simple uniform field from the view point of theoretical investigation [12,16].

For the sake of convenience, the physical quantities that appear in the following are dimensionless, with energy unit $E^* = \pi^2\hbar^2/2m^*d^2$, wave vector unit $k^* = \sqrt{2m^*E^*/\hbar^2}$, length unit $l^* = 1/k^*$, time unit $t^* = \hbar/E^*$, frequency unit $\omega^* = 1/t^*$, and the unit of field amplitude $\varepsilon^* = E^*/el^*$, where d is the width of the leads.

We consider the case when the system has geometry and field parameters such that only the two lowest modes are involved in the electron transport [12]. Assume that an electron with an incident energy E emits from the left lead to the interface at $x = 0$, then transmission and reflection will take place simultaneously. Because the electron has certain probability of absorbing a photon after penetrating the interface into the dot, transition from the lower mode to the upper mode happens. So there are two energy components of E and $E + \hbar\omega$ in the reflection wave in the region of $x < 0$ (see the detailed analysis for the validity of this approximation solution in Ref. [12])

$$\Psi(x,y,t) = [e^{i(k_1x - Et)} + c_1e^{-i(k_1x+Et)}]\phi_1(y) + c_2e^{-i[k_2x+(E+\omega)t]}\phi_2(y), \quad (2)$$

where $\phi_n(y)$ $(n = 1, 2)$ are the transverse eigenfunctions with eigenvalues ϵ_n in the left lead, c_1 and c_2 are the reflection coefficients of the two modes respectively, and the two corresponding wavevectors are

$$k_1 = \sqrt{E - \epsilon_1}, \quad k_2 = \sqrt{E - \epsilon_2 + \omega}. \quad (3)$$

In the region of $x > 0$, we use a unitary transformation [12] and the rotating-wave approximation [20] to solve the time-dependent Schrödinger equation (1). The solution for electron wavefunction is

$$\Psi(x,y,t) = [c_+e^{i(k_+x - Et)} + c_-e^{i(k_-x - Et)}]\phi_1'(y) + [G_+c_+e^{i[k_+x-(E+\omega)t]} + G_-c_-e^{i[k_-x-(E+\omega)t]}]\phi_2'(y), \quad (4)$$

where $\phi_n'(y)$ $(n = 1, 2)$ are transverse eigenfunctions with eigenvalues ϵ_n' in the dot, $c_\pm$ are the transmission coefficients of the two field-spilt modes and the constants $G_\pm = \pm(\sqrt{\gamma^2 + \xi^2} \mp \gamma)/\xi$ (where $\gamma = \omega - (\epsilon_2' - \epsilon_1')$ is the

detuning, and ξ is the two-mode coupling constant). The two field-spilt wavevectors are

$$k_{\pm} = \sqrt{E - \epsilon_1' + \gamma/2 \mp \sqrt{\gamma^2 + \xi^2}/2}. \quad (5)$$

The solution of the Schrödinger equation must obey two conditions at the interface $x = 0$ at all times.

(1) Continuity of the wave function for $y \in [-D/2, D/2]$ in two dimensions:

$$(1 + c_1)\phi_1(y)\vartheta(d/2 - \mid y \mid) = (c_+ + c_-)\phi_1'(y),$$

$$c_2\phi_2(y)\vartheta(d/2 - \mid y \mid) = (c_+G_+ + c_-G_-)\phi_2'(y), \quad (6)$$

where $\vartheta(y)$ is the Heavyside step function.

(2) Continuity of the first derivative of the wave function for $y \in [-D/2, D/2]$ in two dimensions:

$$(1 - c_1)k_1\phi_1(y) = (c_+k_+ + c_-k_-)\phi_1'(y),$$

$$-c_2k_2\phi_2(y) = (c_+G_+k_+ + c_-G_-k_-)\phi_2'(y). \quad (7)$$

These equations can be transformed into equations independent of transverse eigenfunctions by multiplication with $\phi_n(y)$ and $\phi_n'(y)$ respectively, and by integration over the appropriate y range. Using the abbreviations $\rho_{n'n} = \int dy\phi_n'(y)\phi_n(y)$, we can obtain algebraical equations for the coefficients

$$\rho_{11}(1 + c_1) = c_+ + c_-,$$

$$\rho_{22}c_2 = c_+G_+ + c_-G_-,$$

$$\rho_{11}(k_1 - c_1k_1) = (c_+k_+ + c_-k_-),$$

$$-\rho_{22}c_2k_2 = (c_+G_+k_+ + c_-G_-k_-). \quad (8)$$

With the solution of the coefficients in algebraic equations in equation (8), both the transmission and reflection matrix for the left interface (as if without the right interface) can be expressed by

$$t' = \begin{bmatrix} \sqrt{k_+/k_1}\, c_+ & 0 \\ \sqrt{k_-/k_1}\, c_- & 0 \end{bmatrix}, \quad r = \begin{bmatrix} c_1 & 0 \\ \sqrt{k_2/k_1}\, c_2 & 0 \end{bmatrix}. \quad (9)$$

When we consider the electron transmission probability through the whole system, we use the approach recently developed in reference [21] for the symmetric system. This approach needs to derive the total scattering matrix which can be expressed in the transmission matrix and reflection matrix on each interface. The total transmission matrix is just the anti-diagonal submatrix of the total scattering matrix in the symmetrical system case [21].

Because of the similarity of the two interfaces one has not to match the wave functions at the right interface $x = L$, but we need to know the transmission and reflection matrix of electron emitting from right to left for the left interface. In this case the electron wavefunction in the dot region is

$$\begin{aligned}\Psi(x, y, t) = {} & \\ & [c_+^e e^{-ik_+x} + c_-^e e^{-ik_-x} + c_+^r e^{ik_+x} + c_-^r e^{ik_-x} e^{-iEt}\phi_1'(y) \\ & + [c_+^e G_+ e^{-ik_+x} + c_-^e G_- e^{-ik_-x} + c_+^r G_+ e^{ik_+x} \\ & + c_-^r G_- e^{ik_-x}]e^{-i(E+\omega)t}\phi_2'(y), \quad (10)\end{aligned}$$

where $c_{\pm}^e$ are coefficients of electrons emitting from right to left, $c_{\pm}^r$ are associated reflection coefficients. Correspondingly, the electron wavefunction in the region of $x < 0$ is

$$\begin{aligned}\Psi(x, y, t) = {} & c_1^t e^{-i(k_1x + Et)}\phi_1(y) \quad (11) \\ & + c_2^t e^{-i[k_2x + (E+\omega)t]}\phi_2(y),\end{aligned}$$

where c_1^t and c_2^t are the transmission coefficients. These two wavefunctions also satisfy the continuous condition at $x = 0$, with which we can obtain the normalized transmission and reflection matrix r' and t, respectively (here we do not present the detail expressions for them because they are much more complicated than Eq. (9) for t' and r). Consequently, the total transmission matrix through the two interfaces (the whole system) is

$$t_{tot} = S_{12} = t(1 - Xr'Xr')^{-1}Xt', \quad (12)$$

where

$$X = \begin{bmatrix} e^{ik_+L} & 0 \\ 0 & e^{ik_-L} \end{bmatrix} \quad (13)$$

is the transfer matrix between the two interfaces. Therefore, according to Landauer-Büttiker's formulation [22] the total electron transmission probability through the whole system is

$$T = Tr[t_{tot}^{\dagger}t_{tot}]. \quad (14)$$

3 Results and discussion

In this section, we present some numerical examples for exploring the influence of the external field on the quantum transport properties of the system according to equation (14). In the following, we have used parameters corresponding to a high mobility GaAs/Al_xGa_{1-x}As heterostructure [23] with a typical electron density $n \sim 2.5 \times 10^{11}$ cm^{-2} and $m^* = 0.067\ m_e$. The system geometrical parameters are chosen such that the width $d = 3.14(\simeq 80$ nm) for the leads, and the width $D = 6.28(\simeq 160$ nm) and $L = 15(\simeq 382$ nm) for the open quantum dot, which are typical for current experimental fabrication [23]. Therefore, for a hard-wall transverse confining potential the unit of energy $E^* = 0.88$ meV, the length unit $l^* = 25.5$ nm, the time unit $t^* = 7.50 \times 10^{-13}$ s, the frequency unit $\omega^* = 1.33$ THz, and the unit of field amplitude $\varepsilon^* = 34.5$ V/mm. Consequently, the two lowest

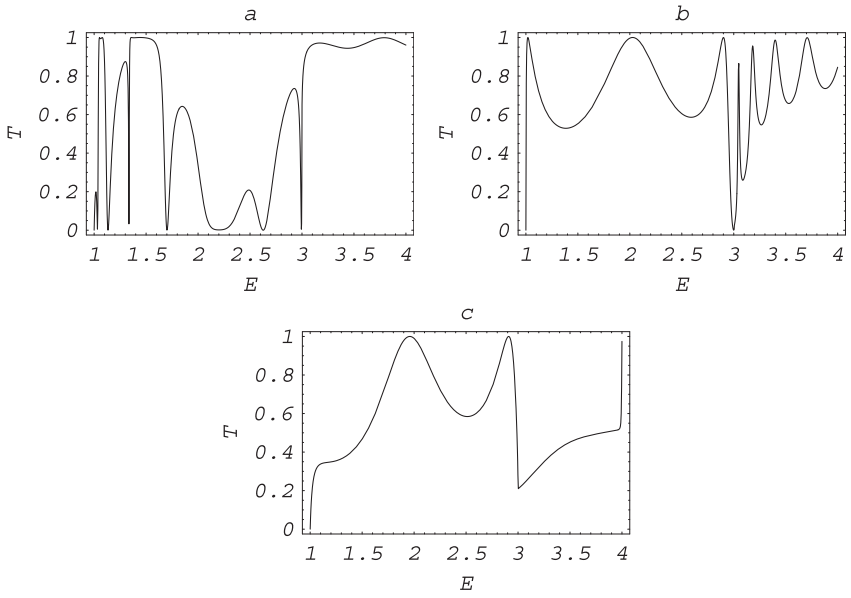

Fig. 2. Transmission probability T as a function of the incident energy E (in units of ϵ_1) with a fixed field frequency $\omega = 1$, for the cases of (a) $\varepsilon = 2$, (b) $\varepsilon = 6.76$, and (c) $\varepsilon = 9$. The geometrical parameters are $d = 3.14$, $D = 6.28$ and $L = 15$ such that $\epsilon_1 = 1$, $\epsilon_2 = 4$, $\epsilon_1' = 0.25$ and $\epsilon_2' = 1$.

subbands are $\epsilon_1 = 1$ and $\epsilon_2 = 4$ for the lead, and $\epsilon_1' = 0.25$ and $\epsilon_2' = 1$ for the dot, respectively.

In the absence of the EM field ($\varepsilon = 0$), the electron transmission pattern was presented in reference [16], which shows three resonant dips. However, when the dot is illuminated by a transversely polarized EM field the transmission is obviously different from the case of time-dependent potential modulation [16]. In Figure 2, we show the calculated transmission probability T as a function of the incident energy E with a fixed field frequency $\omega = 1$ for different ε in the energy window (ϵ_1, ϵ_2). Figure 2a gives an interesting T dependence on E with $\varepsilon = 2$, and we see that the multiple asymmetry Fano dips appear at $E \approx 1.12, 1.34, 1.70, 2.20, 2.62$ and 3.00. The multiple Fano resonances are connected with the interaction of the multiple quasidonor levels appearing above the lowest subband edge and the continuum states [16–18]. In our case the two modes k_+ and k_- in the dot are propagating modes due to the effect of EM field but only one propagating mode (k_1) in the lead. The coupling of k_+ and k_- induces the multiple Fano resonances, which associate with quasi-bound states with $E \leq 3$. With the increase of the incident energy E, mode k_2 begin to be propagating and the transmission is nearly unity. In Figure 2b the interesting dip occurs at $E = 3$ with $\varepsilon = 6.76$. In this case $k_2 = \sqrt{E + \omega - \epsilon_2} \sim 0$ and $k_+ = \sqrt{E - \epsilon_1' + \gamma/2 - \sqrt{\gamma^2 + \xi^2}/2} \sim 0$, then the two modes ($k_2$ and k_+) begin to be propagating simultaneously. The symmetry Breit-Winger resonances appear within $0 < E < 3$ result from the interference of the electron waves in the nonadiabatic geometry structure. Therefore, it is reasonable that the step structure in Figure 2c occur within $3 < E < 3.95$ where the mode k_2 in the lead begin to be propagating earlier than k_+ in the dot. This means that the propagating mode k_2 strengthen the reflection probability of electrons and the transmission is suppressed. From the above results and discussions we can conclude that the rectangular open quantum dot shows an interesting transmission characteristics due to the presence of the external EM field. The two lower modes k_1 and k_- are always propagating. The field parameters can control the propagational property of the two upper modes k_2 and k_+, and then affect the electron transmission.

Next, we separately study the influence of field frequency and amplitude on the transmission probability T with the interesting incident energy $E = 3$. Firstly, the transmission probability T as a function of ω for four ε is shown in Figure 3. In Figure 3a, the coupling of the two propagating modes k_+ and k_- results in the multiple Fano resonances with $\varepsilon = 2$ and $\omega \leq 1$. And the interesting dip structure also occur at $\omega = 1$ with $\varepsilon = 6.76$ as shown in Figure 3b, which implicates that the analysis for Figure 2b is reasonable. With ε increasing to 9 in Figure 3c, mode k_+ in the dot does not open until $\omega = 1.27$. So the propagating mode k_2 in the lead strengthen the reflection of electrons and the transmission is suppressed around $\omega \sim 1$. As the field amplitude increases further, as shown in Figure 3d, the transmission is more suppressed with higher frequencies because in this case there is only one propagating mode k_- in the dot. From the above analysis, we find that whether the second mode k_2 is propagating or not depends on the value of field frequency ω with constant E. But the propagational property of mode k_+ depends on the value of both field frequency ω and amplitude ε. Secondly, we present T dependence on ε for four frequencies of $\omega = 0.5$, 1, 1.2 and 1.7, corresponding to Figure 4a–d respectively. There are still some dip structures on the transmission at lower field amplitudes as shown in Figure 4a. However, as shown in Figures 4b–d, with the increasing of ω, the second mode k_+ begin to be evanescent mode and the transmission is more suppressed.

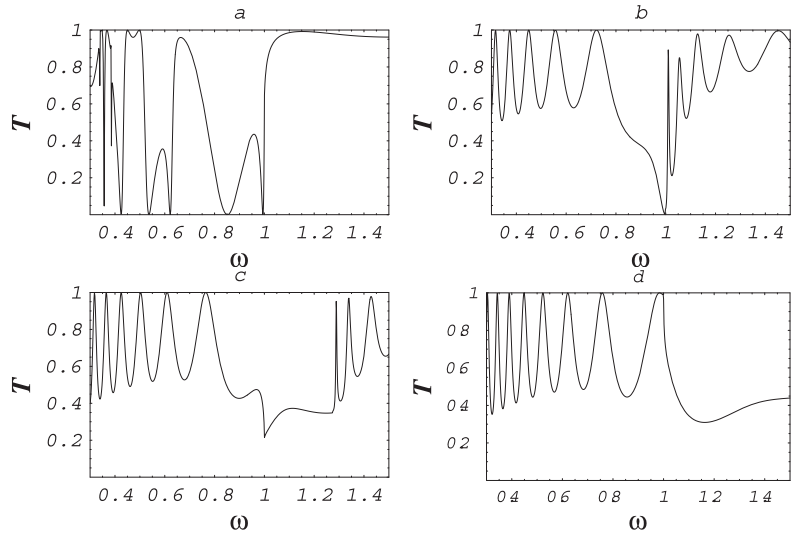

Fig. 3. Transmission probability T as a function of field frequency ω with incident energy $E = 3$, for the cases of (a) $\varepsilon = 2$, (b) $\varepsilon = 6.76$, (c) $\varepsilon = 9$, and (d) $\varepsilon = 11$. The geometrical parameters are the same as in Figure 2.

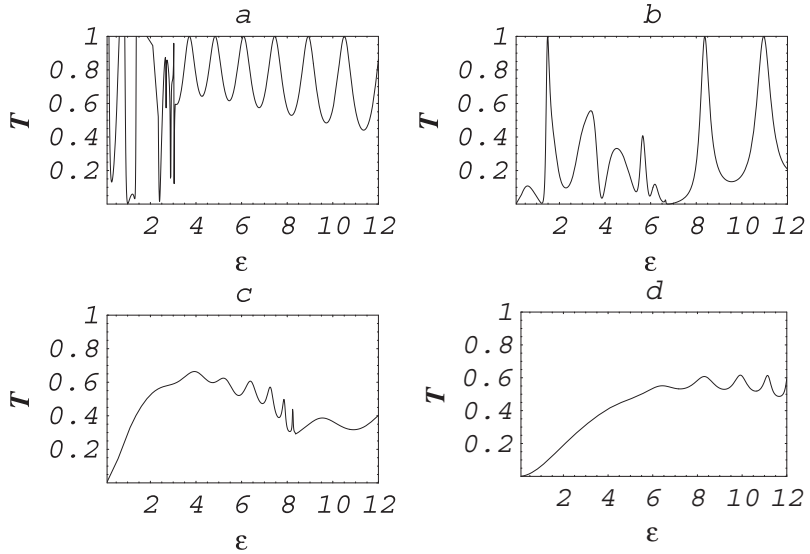

Fig. 4. Transmission probability T as a function of field amplitude ε with incident energy $E = 3$, for the cases of (a) $\omega = 0.5$, (b) $\omega = 1$, (c) $\omega = 1.2$, and (d) $\omega = 1.7$. The geometrical parameters are the same as in Figure 2.

A phase coherent phenomenon by nature resonant backscattering can be destroyed by inelastic relaxation of the photoexcited electrons. The typical excess energy ΔE of electrons corresponds roughly to the energy spacing between lateral levels in the quantum dot. Hence, for a submicron size dot it is of order 10 K. Using inelastic electron relaxation for a high mobility 2DEG in the recent experiments [23], an inelastic mean free path is estimated as $\sim 1\mu$m if $\Delta E \leq$10 K. This is sufficiently long to make the the effects discussed above observable in a realistic experimental situation.

4 Conclusion

Using the free-electron model and the scattering matrix approach via time-dependent mode matching, we have investigated theoretically the electron transport properties through an open rectangular quantum dot illuminated under a transversely polarized external EM field. We have calculated the electron transmission as a function of incident energy and field parameters. Through serval numerical examples we have predicted some interesting field-induced resonance effects. Our results are distinguishable from the previous investigation for the same or similar geometry system in several aspects. Firstly, there are some multiple Fano resonances due to the field-induced coupling between the propagating modes in the dot. Secondly, one dip structure will occur when the second modes in both dot and lead begin to be propagating simultaneously with appropriate external parameters. Thirdly, we have predicted a step structure if the second mode in the lead begin to be propagating earlier than the second mode in the dot. Therefore, we conclude that the field parameters ω and ε can control the characteristics of electron

transmission through the propagational property of the modes in an open quantum dot. These effects of the applied external field on the transport properties may be useful for understanding basic physics of quantum structures and for applications in device physics.

This work was supported by the Nature Science Foundation of Hunan (No. 02JJY2008) and by the Research Foundation of Hunan Eduction Commission (NO. 04A031).

References

1. B.J. van Wees, H. van Houten, C.W.J. Beenakker, J.G. Williamson, L.P. Kouwenhoven, D. van der Marel, C.T. Foxon, Phys. Rev. Lett. **60**, 848 (1988)
2. D.A. Wharam, T.J. Thorton, R. Newbury, M. Pepper, H. Ahmed, J.E.F. Frost, D.G. Hasko, D.C. Peacock, D.A. Ritchie, G.A.C. Jones, J. Phys. C **21**, L209 (1988)
3. B.J. Wees, H. Houten, C.W.J. Beenakker, J.G. Williamson, L.P. Kouwenhoven, M. Mare, C.T. Foxon, Phys. Rev. Lett. **60**, 848 (1998)
4. C.S. Kim, A.M. Satanin, Y.S. Joe, R.M. Cosby, Phys. Rev. B **60**, 10962 (1999); Y.S. Joe, R.M. Cosby, J. Appl. Phys. **81**, 6217 (1997); J. Faist, P. Guéret, H. Rothuizen, Phys. Rev. B **42**, 3217 (1990)
5. O.P. Sushkov, Phys. Rev. B **64**, 155319 (2001)
6. D. Boese, W. Hofstetter, H. Schoeller, Phys. Rev. B **64**, 125309 (2001)
7. F. Hekking, Y.V. Nazarov, Phys. Rev. B **44**, 11506 (1991)
8. L.Y. Gorelik, F.A. Maaϕ, R.I. Shekhter, M. Jonson, Phys. Rev. Lett. **78**, 3169 (1997)
9. M. Wagner, W. Zwerger, Phys. Rev. B **55**, R10217 (1997)
10. Qing-feng Sun, Jian Wang, Tsung-han Lin, Phys. Rev. B **61**, 13032 (2000)
11. S. Blom, L.Y. Gorelik, Phys. Rev. B **64**, 45320 (2001)
12. Guanghui Zhou, Mou Yang, Xianbo Xiao, Yuan Li, Phys. Rev. B **68**, 155309 (2003)
13. J.C. Cao, X.L. Lei, Phys. Rev. B **67**, 85309 (2003)
14. P.F. Bagwell, R.K. Lake, Phys. Rev. B **46**, 15329 (1992); M.H. Pedrsen, M. Büttiker, Phys. Rev. B **58**, 12993 (1998)
15. Wenjun Li, L.E. Reichl, Phys. Rev. B **60**, 15732 (1999)
16. C.S. Tang, Y.H. Tan, C.S. Chu, Phys. Rev. B **67**, 205324 (2003)
17. Mou Yang, Shu-Shen Li, Phys. Rev. B **70**, 4318 (2004)
18. U. Fano, Phys. Rev. **124**, 1866 (1961)
19. C.M. Marcus, A.J. Rimberg, R.M. Wetervelt, P.F. Hopkins, A.C. Gossard, Phys. Rev. Lett. **69**, 506 (1992)
20. D.F. Walls, G.J. Milburm, *Quantum Optics* (Springer-Verlag, Belin, 1994)
21. F. Kassubek, C.A. Stafford, H. Grabert, Phys. Rev. B **59**, 7560 (1999)
22. R. Landauer, Philos. Mag. **21**, 863 (1970); M. Büttiker, Phys. Rev. B **35**, 4123 (1987)
23. A. Yacoby, H.L. Stormer, N.S. Wingreen, L.N. Pfeiffer, K.W. Baldwin, K.W. West, Phys. Rev. Lett. **77**, 4612 (1996); C.T. Liang, M. Pepper, M.Y. Simmons, C.G. Smith, D.A. Ritchie, Phys. Rev. B **61**, 9952 (2000); R. de Picciotto, L.N. Pfeiffer, K.W. Baldwin, K.W. West, Phys. Rev. Lett. **92**, 36805 (2004)